

MATCHED GAUSSIAN MULTITAPER SPECTROGRAM

Maria Hansson-Sandsten

Mathematical Statistics,
Centre for Math. Sciences, Lund University,
SE-221 00 Lund, Sweden,
email: sandsten@maths.lth.se

ABSTRACT

A novel multitaper spectrogram estimator for Gaussian functions is proposed. The multitapers are the Hermite functions and a fixed number of few multitapers are used in the estimate. The weighting factors of the different spectrogram functions are optimized to give the approximative Wigner distribution for the Gaussian function. The performance of the estimator is investigated in terms of resolution and cross-term reduction in the time-frequency domain. Additionally, a simulation example shows the robustness against white noise disturbances. The performance of the new estimator is compared to the Wigner distribution, the usual spectrogram as well as the Choi-Williams and the Born-Jordan distributions.

Index Terms— time-frequency, multitaper, multiple window, Hermite function, Gaussian, matched

1. INTRODUCTION

In the area of time-frequency analysis, a large number of time-frequency distributions have been proposed for different applications. From time-frequency concentration viewpoint, the Wigner distribution is the optimal choice. However, so called cross-terms arise for multi-component signals and these cause severe problems in the interpretation of the Wigner distribution. Today, a huge number of other time-frequency distributions exist with different ability to suppress the resulting cross-terms from the Wigner distribution, [1].

A computationally efficient algorithm that corresponds to a time-frequency distribution can be found using a multitaper spectrogram, especially if the number of averaged spectrograms can be small, [1, 2]. The phrase multitaper (multiple window) was originally introduced for stationary processes in [3]. The Hermite functions are optimal in the aspect of time-frequency localization and orthogonality in the time-frequency domain (in contrast to only considering the frequency domain), [4]. This property has made them to become often used as multitapers for spectrogram estimation of non-stationary signals/processes, [5, 6, 7, 8].

Thanks to the Swedish Research council for funding.

In some contributions, the weighting of the different multitaper spectrograms is optimized for fixed Hermite functions of a model spectrum, [5, 9]. In many practical cases, the spectrum of the signal to be estimated is unknown, but more vague information could be available, e.g., approximate concentration and resolution of time-frequency components.

In this paper, a matched Gaussian function estimator is derived in the time-frequency domain using a fixed number of Hermite functions and optimizing the weighting of the resulting multitaper spectrogram. The theoretical expression for the spectrogram of a Gaussian function windowed with a Hermite function has recently been derived in [10]. The proposed method is evaluated for resolution properties and for disturbances of white noise.

The paper is organized as follows: section 2 introduces the multitaper spectrogram composition of a time-frequency kernel. In section 3, the matched Gaussian multitaper spectrogram is presented and the effect of erroneous scaling of the Hermite functions is investigated. Section 4 evaluates and compares the proposed method with a number of other time-frequency estimators that are well known for good resolution properties and efficient cross-term reduction. The paper is concluded in section 5.

2. THE MULTITAPER SPECTROGRAM

The multitaper spectrogram is defined as

$$S_x(t, \omega) = \sum_{k=1}^K \alpha_k \left| \int_{-\infty}^{\infty} h_k^*(t - t_1) x(t_1) e^{-i\omega t_1} dt_1 \right|^2, \quad (1)$$

where $x(t)$ is the signal and α_k , $k = 1 \dots K$, are the weights. The windows $h_k(t)$, $k = 1 \dots K$, are the Hermite functions, defined as

$$h_k(t) = \frac{1}{\sqrt{\pi^{1/2} 2^{(k-1)} (k-1)!}} H_{k-1}(t) e^{-\frac{t^2}{2}}, \quad k = 1, 2, \dots,$$

where

$$H_k(t) = (-1)^k e^{t^2} \frac{d^k}{dt^k} e^{-t^2}, \quad k = 0, 1, \dots$$

The multitaper spectrogram $S_x(t, \omega)$ can be expressed as the quadratic class of time-frequency distributions, see e.g., p.188 in [1], using $t_1 = t' + \frac{\tau}{2}$ and $t_2 = t' - \frac{\tau}{2}$,

$$Q_x(t, \omega) = \int_{-\infty}^{\infty} \int_{-\infty}^{\infty} r_x(t', \tau) \rho_{MT}(t - t', \tau)^* e^{-i\omega\tau} dt' d\tau, \quad (2)$$

where we identify the instantaneous autocorrelation function

$$r_x(t, \tau) = x\left(t + \frac{\tau}{2}\right)x^*\left(t - \frac{\tau}{2}\right), \quad (3)$$

and the multitaper time-lag kernel

$$\rho_{MT}(t, \tau) = \sum_{k=1}^K \alpha_k h_k\left(t + \frac{\tau}{2}\right) h_k^*\left(t - \frac{\tau}{2}\right) = \sum_{k=1}^K \alpha_k \rho^{h_k}(t, \tau). \quad (4)$$

The Wigner distribution of the signal is

$$W_x(t, \omega) = \int_{-\infty}^{\infty} r_x(t, \tau) e^{-i\omega\tau} d\tau, \quad (5)$$

and the multitaper time-frequency kernel is

$$\begin{aligned} W_{MT}(t, \omega) &= \int_{-\infty}^{\infty} \sum_{k=1}^K \alpha_k \rho^{h_k}(t, \tau) e^{-i\omega\tau} d\tau, \\ &= \sum_{k=1}^K \alpha_k W^{h_k}(t, \omega). \end{aligned} \quad (6)$$

3. A MATCHED GAUSSIAN MULTITAPER SPECTROGRAM ESTIMATOR

A Gaussian windowed signal

$$x(t) = g(t - t_0) e^{-i\omega_0 t}, \quad (7)$$

where the unit-energy Gaussian function is

$$g(t) = \pi^{-\frac{1}{4}} e^{-\frac{1}{2}t^2}, \quad -\infty < t < \infty \quad (8)$$

is often used to model a short non-stationary signal. The quadratic class of distributions obey time-frequency shift-invariance $S_x(t - t_0, \omega - \omega_0) = S_g(t, \omega)$, meaning that the further analysis can be restricted to $x(t) = g(t)$. In [10], the Gabor spectrogram (using a Gaussian window) of a Hermite function, is derived, using the circular symmetry properties of the Gaussian function as well as the Hermite window. Adapting this result, shifting the k :th Hermite function to be the window function and the Gaussian window to be a Gaussian signal, the resulting Hermite function windowed spectrogram for the signal in Eq. (8) is

$$S_g^{h_k}(t, \omega) = \frac{1}{2^{k-1}(k-1)!} (t^2 + \omega^2)^{(k-1)} e^{-\frac{1}{2}(t^2 + \omega^2)}.$$

The Wigner distribution of the Gaussian function is

$$W_g(t, \omega) = 2e^{-(t^2 + \omega^2)}, \quad (9)$$

and it can be shown that

$$W_g(t, \omega) = \sum_{k=1}^{\infty} \alpha_k S_g^{h_k}(t, \omega), \quad (10)$$

if one uses $x = -\frac{1}{2}r^2 = -\frac{1}{2}(t^2 + \omega^2)$, giving Eq. (9) equal to Eq. (10) as

$$2e^{2x} = \sum_{k=1}^{\infty} \alpha_k \frac{1}{(k-1)!} (-x)^{(k-1)} e^x.$$

We find

$$e^x = \frac{1}{2} \sum_{k=1}^{\infty} \alpha_k \frac{1}{(k-1)!} (-x)^{(k-1)},$$

where the terms in the series expansion $e^x = \sum_{n=0}^{\infty} \frac{x^n}{n!}$ with $\alpha_m = 2$ and $\alpha_{m+1} = -2$ for $m = 2k - 1$ can be identified. However, an infinite sum of multitaper spectrograms is of no use in practical calculations, but if the number of terms in the sum is limited, i.e., K in Eq. (1) is assumed to be small, the computational effort would be reasonable.

Fixing K and minimizing the total squared error with respect to $\alpha_k, k = 1 \dots K$,

$$e_{min} = \min_{\alpha_k} \int_t \int_{\omega} \left(\sum_{k=1}^K \alpha_k S_g^{h_k}(t, \omega) - W_g(t, \omega) \right)^2, \quad (11)$$

will give the low-rank approximate Wigner distribution for the Gaussian function as a weighted multitaper spectrogram estimate, with the weights α_k and the Hermite functions $h_k(t)$ as window functions, $k = 1 \dots K$. The proposed method is named Matched Gaussian MultiTaper spectrogram (*MGMT*), presented as *MGMT_K* for the K windows that are chosen.

The resulting weights, for some examples of fixed K , is seen in Figure 1a). For $K = 2$, the resulting weights are $\alpha_1 \approx 2$ and $\alpha_2 \approx -1$ (blue stars). For larger values of K , the resulting weights are closer to the theoretical calculation above for infinite K , i.e., alternating between values closer to 2 and -2 . These weights are applicable for a Gaussian function and corresponding optimal Hermite functions disregarding the scaling of the parameter r . In Figure 1b), the resulting multitaper spectrogram of the Gaussian function, $\sum_{k=1}^K \alpha_k S_g^{h_k}(t, \omega)$ for different values of K (blue, green and red solid lines) are shown together with the true Wigner distribution $W_g(t, \omega)$, (cyan dashed line) for $r = \sqrt{t^2 + \omega^2}$. It is seen that also for low values of K , $K = 2$ and 3, the multitaper spectrogram is a close approximation to the Wigner distribution.

The *MGMT* spectrogram gives a small error when the optimal Hermite functions are used. However, in a practical application, the scaling of the Hermite windows has to be

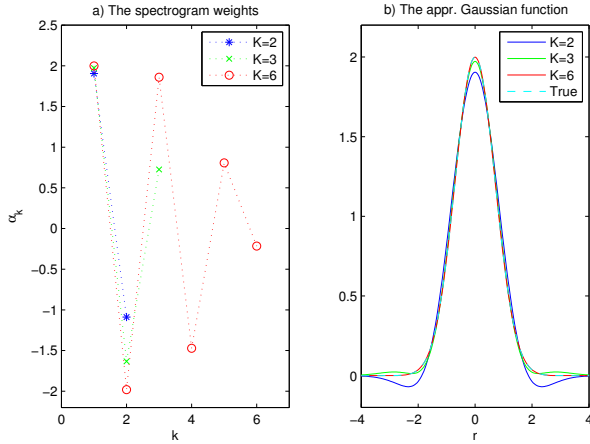


Fig. 1. a) The resulting weights of the $MGMT_K$ spectrogram for different fixed values of K ; b) the corresponding $MGMT_K$ spectrograms of the Gaussian function for the different values of K together with the true Wigner distribution $W_g(t, \omega)$ for $r = \sqrt{t^2 + \omega^2}$.

given from some a priori information or estimated from data. This might cause certain errors in the final estimate. We investigate how different scaling of the Hermite functions effect the final error, when applied as windows together with the optimal weights. The result is seen in Figure 2 where the average squared errors of the $MGMT$ spectrogram for different fixed values of K are plotted when the set of Hermite functions are erroneously scaled compared to the Gaussian function to be estimated. The error is calculated as the average over the total time-frequency domain and the test signal is the 128 sample complex-valued low-frequency component of the signal shown in Figure 3. The scale on the x-axis of Figure 2 is given as r_g/r_h where r_g represents the scale of the Gaussian function and r_h the scaling of the set of Hermite functions used in the estimation. The smallest errors are, as expected, given for $r_g = r_h$ but the effect of erroneous scaling of the Hermite functions are not very large, which indicates that the estimator would perform rather well also when the scaling of the Gaussian function is unknown or estimated.

4. EVALUATION

The $MGMT$ spectrogram is compared with some quadratic class methods that are well known for good resolution properties and efficient cross-term reduction. The test signal is given as two complex valued Gaussian components that are moved closer together in time as well as in frequency. The signal is exemplified in Figure 3, where the first component is located at $n = 128$ and $\omega = 2\pi \cdot 0.1$ and the second at $n = 288$ and $\omega = 2\pi \cdot 0.15$, ($\omega = 2\pi f$), i.e., the time difference is $\Delta t = 160$ and the frequency difference is $\Delta f = 0.05$. Each component

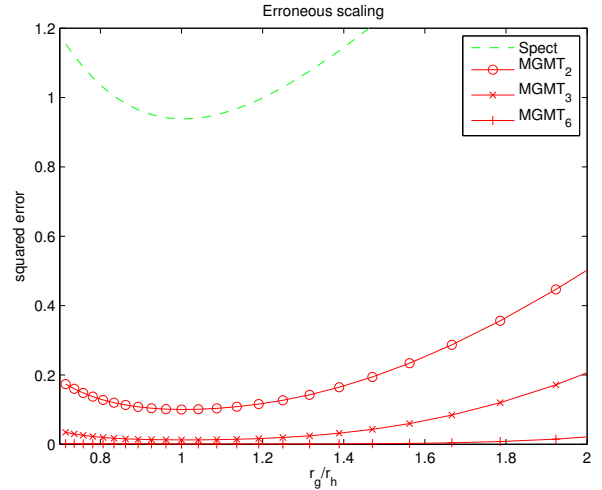


Fig. 2. The mean squared error for erroneous scaling of the Hermite functions used as window functions of the $MGMT_K$ spectrogram. The scale on the x-axis is given as the ratio between the scale r_g of the Gaussian function to be estimated and the scale of the Hermite functions r_h .

is of length 128 samples. The *sum of the Wigner distributions of the two individual components* are used as the true spectrum in the comparisons. In the calculations, the signal is 512 samples long and the number of FFT-samples is 1024.

The two components are moved closer to each other in time- as well as in frequency and the squared error between the true spectrum and the estimate of the sum of the two components using the different methods. The mean of the error is calculated for all (512 X 1024) values in the time-frequency grid. The results are shown in Figure 4, where the $MGMT_K$ spectrograms of fixed value $K = 2, 3$ and 6 are compared to the Choi-Williams distribution, [11], for different values of the exponential decrease (exp.d.) parameter, and to the Born-Jordan (Sinc) distribution, see e.g., [1]. Both of these methods are well known to reduce cross-terms and keep auto-term resolution. The unweighted spectrogram, using the optimal first (unit-energy) Hermite function as window, is also included in the comparison. The Wigner distribution of the sum of the components are not included in the figure as this value is many times larger than the axis shown, due to the cross-term between the two components, (mean squared error ≈ 15).

It is clearly seen that the error for the $MGMT$ spectrogram (red lines) is superior to the other methods when the components are further away from each other. Especially does $K = 6$ and $K = 3$ give a better result than the Choi-Williams distribution (blue dashed lines, 2 different exp.d. values, 0.05 and 0.2) as well as the Born-Jordan distribution (dotted pink line). The spectrogram (green dash-dotted line) gives the largest error. For components that are closer together than $\Delta f = 0.04$ and $\Delta t = 128$, the $MGMT_2$

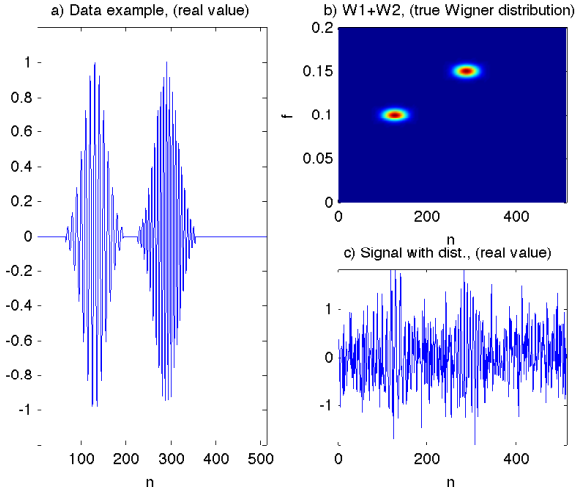


Fig. 3. Example of the test signal with two complex valued Gaussian components where $\Delta t = 160$ and $\Delta f = 0.05$; a) The real value of the time-signal; b) the sum of the Wigner distributions of the two components, which is used as the true signal in the comparison; c) the test signal with white noise disturbance of standard deviation $\sigma = 0.5$.

gives a similar result as the Born-Jordan distribution, where $MGMT_3$ and $MGMT_6$ give larger errors.

4.1. White noise disturbance

To investigate the robustness of the $MGMT$ spectrogram against disturbances, a white complex valued circular Gaussian noise disturbance of standard deviation σ is added to the test signal with parameters $\Delta t = 160$ and $\Delta f = 0.05$ presented in Figure 3. A number of 100 simulations is made for different realizations of the noise. The phase of the sinusoidal Gaussian components of the test signal is also varied for each realization, uniformly distributed between $-\pi$ and π . The mean error of the squared bias and the variance of the low-frequency component is calculated close around the component, for time interval $t = 32$ to 224 and frequency interval $f = 0.075$ to 0.125 . The results of the different methods are shown in Figure 5. The mean of the squared bias in the time-frequency grid around the components is presented in Figure 5a) and the mean of the variances for the same grid is presented in Figure 5b). The squared bias of the $MGMT$ spectrograms (red solid lines) are the smallest compared to all the other methods and we can see that the bias of the $MGMT_6$ is small for moderate disturbances but for larger values of σ , the smallest error is given by the $MGMT_2$ spectrogram. The variance of the $MGMT$ spectrogram is however larger than the usual spectrogram (green dash-dotted line) as well as the Choi-Williams distribution (exp.d.=0.05) (dashed circled blue line) and give comparable results to the Born-Jordan kernel and the Choi-Williams kernel (exp.d.=0.2) (dotted pink line

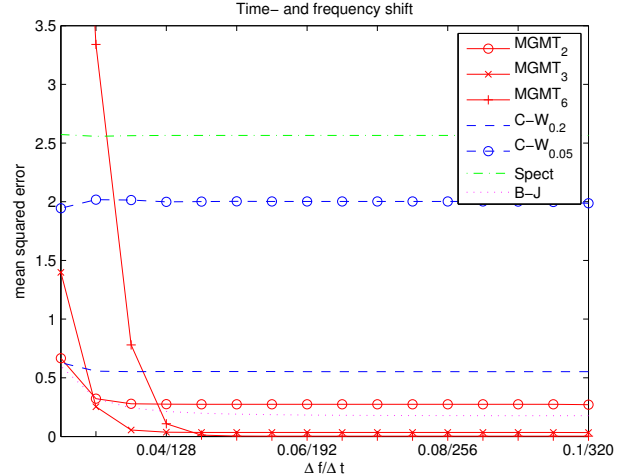


Fig. 4. The resulting mean squared error of different methods comparing to the true Wigner spectrum in Figure 3 when the components are moved closer in time- as well as frequency.

and dashed blue line), Figure 5b). The squared bias and the variance are added together resulting in the mean squared error and the mean value over the time-frequency grid is presented in Figure 6. For small to moderate disturbances, $\sigma \leq 0.5$, (see example of moderate disturbance $\sigma = 0.5$ in Figure 3c)), the performance of the $MGMT$ spectrogram is the best, where the $MGMT_3$ or $MGMT_6$ should be favored in the case of small disturbances. For larger values of σ , the spectrogram gives the smallest error, but the $MGMT$ spectrogram is still comparable to the Choi-Williams and Born-Jordan distributions.

5. CONCLUSION

A matched Gaussian multitaper ($MGMT$) spectrogram that gives the approximate Wigner distribution for a Gaussian function is proposed. The number of Hermite function windows to be used in the estimate is fixed and then the weights of the windowed spectrograms are optimized. The resolution and cross-term reduction performances of the new estimator is investigated showing that the performance is very high for components that are well-resolved in the time-frequency domain. For closer components, the performance for $K = 2$ windows ($MGMT_2$) is similar to the Born-Jordan distribution. The performance for white noise disturbances is also investigated, showing that $K = 3$ windows ($MGMT_3$) is better than the Born-Jordan distribution for small and moderate disturbances in the mean square error sense (MSE) and still comparable for large disturbances. For large disturbances the usual spectrogram gives the smallest MSE, followed by the Choi-Williams distribution, (exp.d.=0.05), and the $MGMT_2$.

In summary, the proposed estimator is easily computed

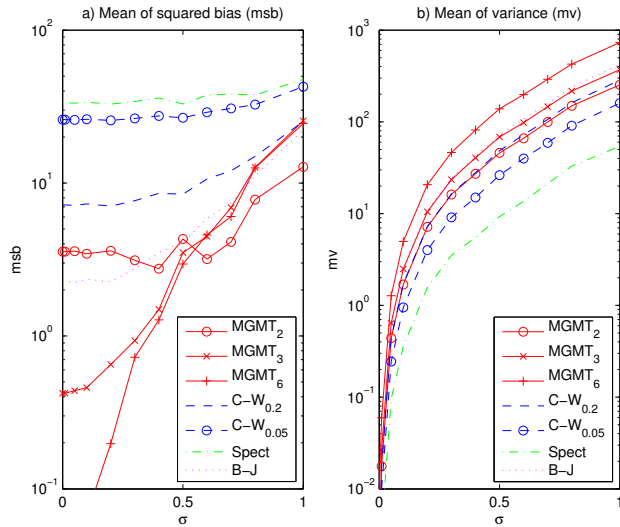


Fig. 5. Example of the performance for the test signal with two Gaussian components, and white noise disturbance for different values of the standard deviation σ ; a) the mean of the squared bias in the time-frequency grid; b) the mean of the variances in the time-frequency grid. The mean is calculated around the low frequency component.

using the Hermite functions as windows and the average of a small number (2 or 3) of resulting weighted spectrograms, where the weighting factors are independent of the scaling of data and window functions. The resulting multitaper spectrogram estimator has a high performance both in resolution as well as robustness against noise disturbances.

6. REFERENCES

- [1] L. Cohen, *Time-Frequency Analysis*, Prentice-Hall, 1995.
- [2] M. G. Amin, "Spectral decomposition of time-frequency distribution kernels," *IEEE Trans. on Signal Processing*, vol. 42, no. 5, pp. 1156–1165, May 1994.
- [3] D. J. Thomson, "Spectrum estimation and harmonic analysis," *Proc. of the IEEE*, vol. 70, no. 9, pp. 1055–1096, Sept 1982.
- [4] I. Daubechies, "Time-frequency localization operators: A geometric phase space approach," *IEEE Trans. on Information Theory*, vol. 34, no. 4, pp. 605–612, 1988.
- [5] F. Cakrak and P. J. Loughlin, "Multiple window time-varying spectral analysis," *IEEE Trans. on Signal Processing*, vol. 49, no. 2, pp. 448–453, 2001.

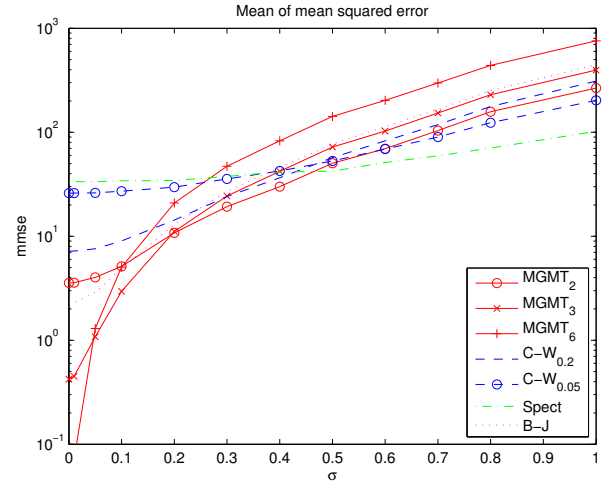


Fig. 6. Example of the performance for the test signal with two Gaussian components, and white noise disturbance for different values of the standard deviation σ . The mean of the mean squared error is calculated over the time-frequency grid of the low-frequency component.

- [6] S. Aviyente and W. J. Williams, "Multitaper marginal time-frequency distributions," *Signal Processing*, vol. 86, pp. 279–295, 2006.
- [7] P. Wahlberg and M. Hansson, "Kernels and multiple windows for estimation of the Wigner-Ville spectrum of gaussian locally stationary processes," *IEEE Trans. on Signal Processing*, vol. 55, no. 1, pp. 73–87, January 2007.
- [8] M. Hansson-Sandsten, "Optimal estimation of the time-varying spectrum of a class of locally stationary processes using Hermite functions," *EURASIP Journal on Advances in Signal Processing*, 2011, Article ID 980805.
- [9] M. Hansson-Sandsten and J. Sandberg, "Optimization of weighting factors for multiple window spectrogram of event related potentials," *EURASIP Journal on Advances in Signal Processing*, 2010, Article ID 391798.
- [10] P. Flandrin, "A note on reassigned Gabor spectrograms of hermite functions," *J Fourier Analysis and Applications*, 2012, DOI 10.1007/s00041-012-9253-2.
- [11] H.-I. Choi and W. J. Williams, "Improved time-frequency representation of multi-component signals using exponential kernels," *IEEE Trans. on Acoustics, Speech and Signal Processing*, vol. 37, pp. 862–871, June 1989.